Eur. J. Mineral.
2003, **15**, 589–598

Characterization of basic cancrinite synthesized in a butanediol-water system

MICHAEL FECHTELKORD[1]*, BRITTA POSNATZKI[2] and JOSEF-CHRISTIAN BUHL[2]

[1]Institut für Geologie, Mineralogie und Geophysik, Ruhr-Universität Bochum, Universitätsstr. 150, D-44780 Bochum, Germany
*Corresponding author, e-mail: Michael.Fechtelkord@ruhr-uni-bochum.de
[2]Institut für Mineralogie, Universität Hannover, Welfengarten 1, D-30167 Hannover, Germany

Abstract: Na-cancrinite [ideal composition: $Na_8(AlSiO_4)*(OH)_2*8H_2O$] has been synthesized in a mixture of 1,3- or 1,4-butanediol and water either with direct reactants (silica sources: tetraethoxysilane, precipitated silica, alumina sources: aluminium sec-butoxide) or gels formed from tetraethoxysilane and aluminium sec-butoxide / aluminium isopropoxide with sodium hydroxide as mineralizing agent. The products were characterized by X-ray powder diffraction and FTIR spectroscopy at room temperature and elevated temperatures up to 1073 K, coulometric and carbon titration, thermogravimetry, scanning electron microscopy and ^{29}Si, ^{23}Na and ^{27}Al MAS NMR spectroscopy, as well as ^{1}H and $\{^{1}H\}^{13}C$ CPMAS NMR spectroscopy. The X-ray powder patterns show cancrinite as the only phase in all samples. The spectroscopic and analytic investigations mainly suggest the presence of both molecular water and hydroxyl anions beside small impurities of carbonate. X-ray diffraction of all samples at elevated temperatures indicates decomposition temperatures in the range between 933 and 1003 K. The structure refinement of a selected sample in the hexagonal space group $P6_3$ reveals a hydroxylcancrinite with lattice parameters $a_0 = 12.7558(3)$ Å and $c_0 = 5.1985(2)$ Å with $R_p = 0.0107$, $R_{wp} = 0.0161$, and $R(F^2) = 0.0373$. The structure is characterized by water molecules and hydroxyl anions occupying two 6c positions and one 2a position, coordinating sodium in the channel.

Key-words: cancrinite, organic solvents, characterization, NMR spectroscopy, Rietveld structure refinement.

Introduction

The cancrinite crystal structure is formed by layers of six-membered rings called the secondary building units SBU-6 in zeolite nomenclature (Meier & Olson, 1992). The edges of the six-membered rings of these two-dimensional layers are occupied by corner sharing aluminium and silicon tetrahedra in an alternating manner connected by oxygen atoms. Stacking these layers in an ABAB sequence leads to the cancrinite framework with its two main structural features: the ε-cages and the large twelve-membered ring channel. The hexagonal structure in space group $P6_3$ is characterized by the periodic arrangement of the ε-cages which form generally an infinite one-dimensional twelve-membered ring channel along the crystallographic c-axis, with a diameter of 5.9 Å (Meier & Olson, 1992). In principle these characteristic features should enable technical applications for several purposes, *e.g.*, using the hexagonal channel for one-dimensional ion conduction or polarizing optical properties.

However, compared to numerous structural investigations (Jarchow, 1965; Barrer *et al.*, 1970; Grundy & Hassan, 1982; Nadezhina *et al.*, 1991 and Kanepit & Rider, 1995) application-oriented work is rarely found in the literature. Lindner *et al.* (1995) investigated the properties of thiosulphate in a cancrinite matrix. They showed that during annealing of the cancrinite S_2^- and S_3^- radicals were formed producing a characteristic yellow to green-blue colour which was explained by an alignment of the radical anions along the channel. Further investigations dealt with the inclusion of one-dimensional chains of selenium in the channel (Koslov *et al.*, 1989; Bogomolov *et al.*, 1992; Poborchii *et al.*, 1994; Barnakov *et al.*, 1995; Linder *et al.*, 1996). Koslov *et al.* (1989) studied the dielectric and pyroelectric properties of cancrinite in a temperature range of 4.2–500 K and suggested three different dielectric relaxation processes in the temperature interval. Bogomolov *et al.* (1992) discovered the linear alignment of selenium chains in the cancrinite channel using spectroscopic methods and assigned two-dimensional semiconductor properties to the material. Furthermore, Linder *et al.* (1996) showed that the high optical anisotropy of selenium containing cancrinite generates strong polarization effects in UV/VIS and Raman spectra.

In general the channels in cancrinite are blocked by inorganic guest anions, so that useable zeolitic crystal properties for technical applications are missing (Barrer *et al.*, 1970). The approach to remove the guest components by annealing of the guest anion containing cancrinites (*e.g.*, carbonate) has failed, because the decomposition of the guest components is accompanied by the destruction of the framework (Buhl, 1991). Probably, hydroxylcancrinite could be regard-

DOI: 10.1127/0935-1221/2003/0015-0589
0935-1221/03/0015-0589 $ 4.50

ed as a suitable material with zeolitic properties. The hydroxyl anions and water molecules in the channel may be removed under mild conditions (Barrer *et al.*, 1970; Pahor *et al.*, 1982 and Hassan & Grundy, 1991).

Water is the "classic solvent" for zeolite syntheses, but recent studies have increasingly focused on the use of non-aqueous solvents (Liu *et al.*, 1993; Milestone *et al.*, 1995; Burton *et al.*, 1999). In some cases, organic solvents can influence the phase formation according to a structure directing role in addition to a solvating role (Bibby & Dale, 1985). The addition of organic solvents in the hydrothermal synthesis changes the viscosity and polarity of the medium and affects the crystallization process. The higher viscosity and lower polarity of many non-aqueous solvents can reduce convection currents, decrease "hydration" of the reactants, and influence diffusion rates, therefore giving rise to slower mass transfer. Another advantage in the use of organic solvents is that included or surface-covering organic molecules can be easily removed by calcination which provides a "template-free" structure, with a maximum adsorption capacity (Schüth, 1995).

The use of 1,3- and 1,4-butanediol for the synthesis of cancrinite in non-aqueous media was reported by Liu *et al.* (1993), Milestone *et al.* (1995), and recently by Burton *et al.* (1999). They noticed that cancrinite is formed preferentially if molecules of a certain size are present in the non-aqueous solvent. 1,3- and 1,4-butanediols are suitable because they possess an appropriate molecular size. Moreover, they reported an increased Si/Al ratio of 2.5–10 of the cancrinite product.

Another approach of controlling the reaction pathway is the introduction of sol-gels into the synthesis. Sol-gels have a well-connected network, which dissolves very slowly during synthesis. Subsequently, sol-gels favour kinetic controlled reactions rather than thermodynamically controlled ones (Fechtelkord *et al.*, 2001a). The addition of water plays another important role, because it influences the polarity and viscosity of the organic solvent as well as the mobility of the mineralizor OH^- (Fechtelkord *et al.*, 2001a).

The aim of our work is the spectroscopic and structural characterization of four different cancrinite samples synthesized from direct reactants or sol-gels in a solvent composed of 1,3- or 1,4-butanediol and 50% by volume of water as a solvent. The products have been investigated by X-ray powder diffraction and FTIR spectroscopy at room temperature and elevated temperatures up to 1073 K, coulometric and Karl-Fischer titration, thermogravimetry, scanning electron microscopy and ^{29}Si, ^{23}Na and ^{27}Al MAS NMR spectroscopy as well as ^{1}H and $\{^{1}H\}^{13}C$ CPMAS NMR spectroscopy. Our study is the first comprehensive characterization of this material. Synthesis conditions and different silica and alumina reactants, as well as the introduction of sol-gels and the influence of water in the cancrinite synthesis in butanediol, have been extensively investigated in a recent work (Fechtelkord *et al.*, 2001a). The carbon content of the as-synthesized cancrinites is lower and the ability to assimilate water is higher then previously investigated cancrinites synthesized in this system (Liu *et al.*, 1993; Milestone *et al.* 1995; Burton *et al.*, 1999). The crystal structure derived from Rietveld powder data refinement indicates that a hydroxylcancrinite with high water content has been formed. Thus, this is the first time that a carbonate-free hydroxylcancrinite with zeolitic properties is reported here. The structure is similar to the structure of a synthetic Cs-Li cancrinite we have studied recently (Fechtelkord *et al.*, 2001c), but differs from the structure published by Burton *et al.* (1999).

Experimental

Synthesis

The first two samples were synthesized by a direct reaction of the chemical compounds. For sample A1, 3.22 g tetraethoxysilane ($C_8H_{20}O_4Si$, TEOS; FLUKA 86578) and 1.26 g aluminium sec-butoxide ($C_{12}H_{27}AlO_3$, FLUKA 06190) were used. For sample C1 3.0 g precipitated silica (SiO_2, FLUKA 833340) and 2.5 g aluminium sec-butoxide were used. In both syntheses the silica sources and the alumina source had a ratio of Si/Al = 5, to obtain a Si/Al ratio larger than unity for the cancrinite product and given into 20 mL 1,3-butanediol ($C_4H_8(OH)_2$, FLUKA, 18940) with 50 % water (by volume). 2.0–3.0 g sodium hydroxide (NaOH, FLUKA 71691) was introduced as mineralizing agent in both syntheses, respectively.

A second approach used sol-gels. Molar amounts of TEOS and aluminium sec-butoxide (sample O1) or aluminium isopropoxide (sample O2) were dissolved in an ethanol/water-mixture (volume ratio 1:2) with a Si/Al ratio of five (Fechtelkord *et al.*, 2001a). Then a basic hydrolysis was initialized by the addition of a saturated aqueous ammonium hydroxide solution (25 wt% NH_3(aq), MERCK 105426). The solution was stirred for 15 min and left without stirring for another 24 h. The resulting gel was then dried first at 313 K, then at 353 K for 24 h, and finally, at 393 K for 48 h. The dried gel was ground in a mortar before introduction into the main synthesis. In the synthesis, 2 g of the dried gels were given into 20 mL 1,3- or 1,4-butanediol ($C_4H_8(OH)_2$, FLUKA 18960) with 50 % water by volume (20 mL volume of solvent in total) and 2.0–3.0 g sodium hydroxide.

The organothermal synthesis was carried out at the described temperature (Table 1) and autogeneous pressure in 50 mL Teflon coated steel autoclaves under static conditions. The products were washed with acetone to remove organic residues and 500 mL deionized water and dried overnight at 353 K. Sample numbers, synthesis conditions, and products are summarized in Table 1.

Characterization

The qualitative powder diffraction patterns were recorded on a Philips PW 1800 diffractometer (Cu$K_{\alpha 1/\alpha 2}$, 40 kV, 40 mA). The powder diffraction data at elevated temperatures were obtained on a Bühler-camera (Mo$K\alpha_1$) in Bragg-Brentano geometry using a Stoe STADI P diffractometer in a temperature range of 296 K to 1073 K (heating rate: 10 K per minute). A 2θ range of 7 to 17° and a step width of 0.003° were used. Lattice parameters were determined from the reflections by least-squares refinement. The structure re

Table 1. Sample numbers, reactants, solvents, base concentrations, synthesis time and products formed.

No.	Reactants	solvent†	NaOH (g)	synthesis - temperature (K)	synthesis - time (h)	product*
A1	TEOS + Al sec-butoxide	1.3	2.0	393	48	CAN
C1	precipitated silica + Al sec-butoxide	1.3	3.0	393	60	CAN
O1	sol-gel (TEOS + Al sec-butoxide)	1.3	2.0	393	48	CAN
O2	sol-gel (TEOS + Al iso-propoxide)	1.4	2.0	393	24	CAN

*CAN: cancrinite

†1,3- or 1,4-butanediol

finement was based on the powder diffraction pattern of sample C1. The data were recorded in transmission geometry on a Siemens D5000 diffractometer using a focusing germanium (111) monochromator with Cu$K_{\alpha 1}$-radiation. A 2θ range of 7 to 97°, a PSD-step width of 0.00777°, a sample time of 27 s per step, and a total exposure time of 87 hours was used. Rietveld powder refinement calculations were carried out using the GSAS PC-program (Larson & von Dreele, 1985). The structure was drawn with the structure program DIAMOND (Brandenburg, 2001).

Infrared spectroscopy was carried out on a Bruker IFS66v/s FT IR spectrometer (KBr pellets) in order to obtain information about included anions, water molecules, and impurities such as carbonate or adsorbed organic solvents. Furthermore, IR spectra were taken at elevated temperatures up to 923 K. The heating device was a self-built oven with external temperature control attached to the sample chamber of the IFS 66v/s. Data acquisition was carried out in 10 K steps with a heating rate of 3 K per minute and a hold time of 3 minutes before data acquisition.

Thermogravimetric analyses were performed in air between room temperature and 1273 K on a Netzsch STA 429 thermal analysis system equipped with a thermogravimetric analyzer and differential thermoanalysis. The heating rate was 10 K per minute. Internal standard was Al_2O_3.

Coulometric titration of carbon was performed on a Deltronik DELTROMAT 500 electronic titrator with an integrated oxidation furnace. The products were washed with acetone and water, centrifuged and washed again several times to make sure that the estimation of carbon was not affected by surface covering polymerized solvent residues and/or carbonate (from adsorbed carbon dioxide). Scanning imaging was performed using a Philips XL30 instrument operating at 15 kV at the Department of Earth and Ocean Sciences (University of British Columbia, Vancouver).

The NMR spectra were recorded on a BRUKER ASX 400 NMR spectrometer. ^{29}Si MAS NMR measurements were performed using a standard BRUKER 7 mm MAS probe at 79.49 MHz with a single pulse duration of 2 µs (30°

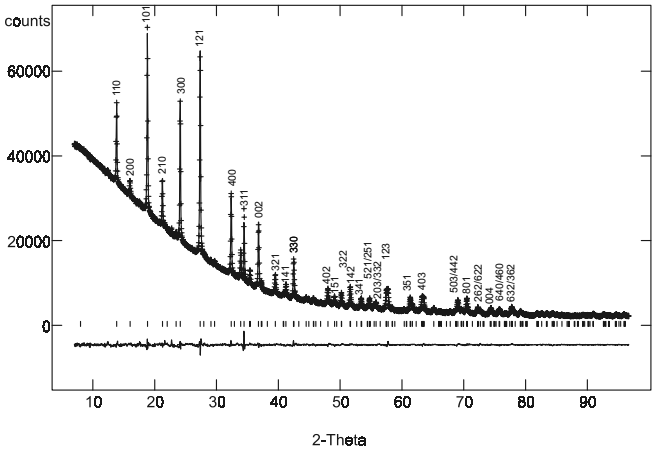

Fig. 1. X-ray powder diffraction pattern of sample C1. The difference pattern of the Rietveld refinement and the Bragg reflection positions are shown below.

Table 2. Lattice parameters, water and carbon contents, and decomposition temperatures (determined by X-ray powder diffraction) of the cancrinite samples. E.S.Dś are given in parentheses.

No.	Lattice parameters		Weight-loss* wt%		carbon content	decomposition temperature
	a_0 (Å)	c_0 (Å)	<1000 K	>1000 K	wt% C	T (K)
A1	12.7043(34)	5.1892(15)	9.0(2)	9.2(2)	0.357(2)	973
C1	12.7021(34)	5.1660(15)	6.8(2)	7.3(2)	0.328(2)	943
O1	12.7243(45)	5.2029(20)	7.9(2)	8.3(2)	0.265(1)	1003
O2	12.7046(41)	5.1720(20)	8.3(2)	8.4(2)	0.281(1)	933

*estimated by thermogravimetry.

tip angle) and a 10 s recycle delay. A total of 800 scans were accumulated at a spinning frequency of 3.5 kHz. Tetramethylsilane has been used as an external standard. The {^{1}H}^{13}C cross-polarization experiments at 100.63 MHz with contact times of 5 ms and 5 s repetition time were carried out using the same 7 mm MAS probe rotating at 3.5 kHz (30,000 scans). The ^{1}H, ^{27}Al and ^{23}Na MAS NMR experiments were obtained at 400.13 MHz, 104.26 MHz, and 105.85 MHz, respectively in a 4 mm standard BRUKER MAS probe. Typical pulse lengths and recycle delays were 0.6 µs and 100 ms for ^{27}Al and ^{23}Na, and 1.5 µs and 5 s for ^{1}H, respectively. A total of 10,000 scans were accumulated at a MAS rotation frequency of 12 kHz for the ^{27}Al and ^{23}Na MAS NMR spectra and a total of 100 scans at the same rotation frequency for the ^{1}H MAS NMR spectra.

Results and discussion

X-ray powder diffraction

The X-ray powder patterns clearly show the formation of cancrinite as the only phase in all four samples. As an example the X-ray powder pattern of sample C1 is given in Fig. 1. Lattice parameters of the hexagonal crystal structure were

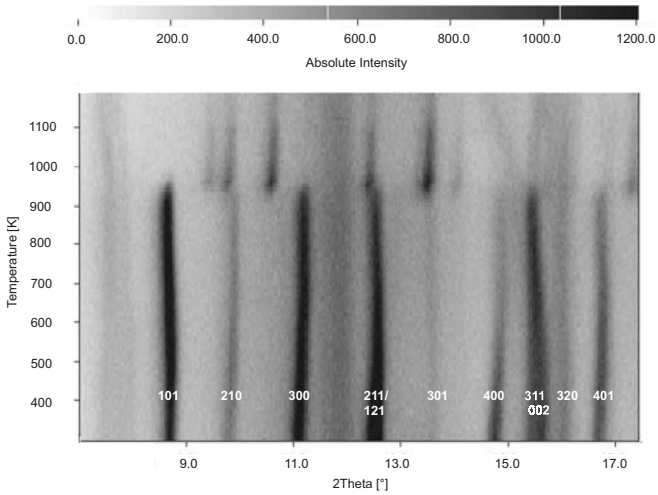

Fig. 2. X-ray powder pattern of sample O2 at variable temperatures.

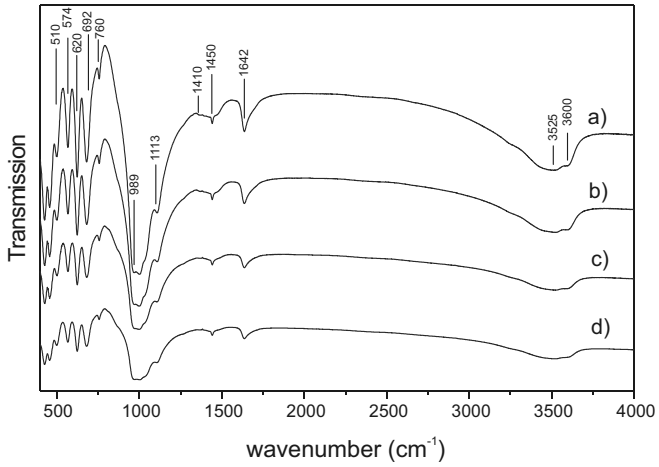

Fig. 3. IR spectra of a) sample A1, b) sample C1, c) sample O1 and d) sample O2 at 296 K.

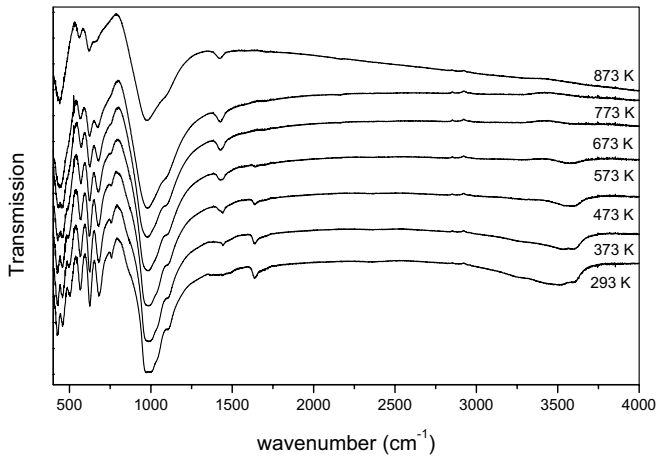

Fig. 4. IR spectra of sample O2 at variable temperatures.

determined by least-squares refinement and are given in Table 2. The low intensity and large halfwidth of the reflections can be attributed to the small grain size (≈2 µm) as observed in the scanning electron micrographs (Fig. 6). The powder patterns of the four samples are similar, except for some intensity and peak position variations, due to diverging lattice parameters and water content (Table 2).

The acquisition of the X-ray powder pattern of sample O2 at elevated temperatures is shown in Fig. 2 as an example. The other three samples displayed a similar behaviour. The data were measured in a 2-theta range of 7-17° with Mo$K_{\alpha 1}$ radiation. At room temperature eight strong reflections can be observed, which are (101), (210), (300), (211)/(121), (301), (400), (311)/(002), (320) and (401). The (400) reflection shows decreasing intensity with increasing temperature and all reflections shift to lower 2-theta values. These changes are induced by loss of crystal water which affects the lattice parameters and intensities of the reflections. The loss of water in this temperature range can also be observed in the IR spectra collected at various temperatures and the TG-analyses. The decomposition of the framework takes place at temperatures between 943 K and 1003 K. The X-ray powder patterns of the other three samples at elevated temperatures showed similar behaviour but different decomposition temperatures. The decomposition temperatures estimated from the X-ray powder data are listed in Table 2. Above this temperature only weak reflections from a nepheline-like phase can be observed (Fig. 2).

IR-spectroscopy

The IR spectra at room temperature for all four samples are very similar. Fig. 3 shows the typical spectral patterns. Asymmetric and symmetric T-O-T vibrations of the cancrinite framework (T = Si, Al) reveal three typical resonance bands in the mid-infrared spectrum at 574, 620, and 692 cm^{-1} (Flanigen *et al.*, 1971). Water molecules, which are adsorbed in the cancrinite channel and in the ε-cages, show a signal at 1642 cm^{-1} (Hackbarth *et al.*, 1999). The absorption band at 1410 cm^{-1} indicates enclathrated impurities of carbonate. Depending on the hydrogen-bonding of the CO_3^{2-} group to the water molecules in the channel a lowering of the threefold symmetry leads to a splitting of the stretching vibration (1450 cm^{-1}). In addition water causes a broad resonance in the range of 2800–3800 cm^{-1} (3525 cm^{-1}). Hydroxyl anions cause a weak, narrow absorption band at 3600 cm^{-1}.

Loss of water occurs between 373 and 773 K, is clearly observed in heating experiments on sample O2 (Fig. 4). The intensity of the water absorption band at 1642 cm^{-1} and at 3525 cm^{-1} decreases continuously as temperature increases. The splitting of the carbonate absorption bands (1410 cm^{-1} and 1450 cm^{-1}) vanishes because the higher molecular symmetry is recovered, due to dehydration. The decomposition of the framework structure can be observed at a temperature of 933 K. The other three samples show a similar spectral pattern at elevated temperatures.

Coulometric titration and estimation of carbon content

It is important to estimate to what extent the structure can be regarded as a template-free structure and to check the car-

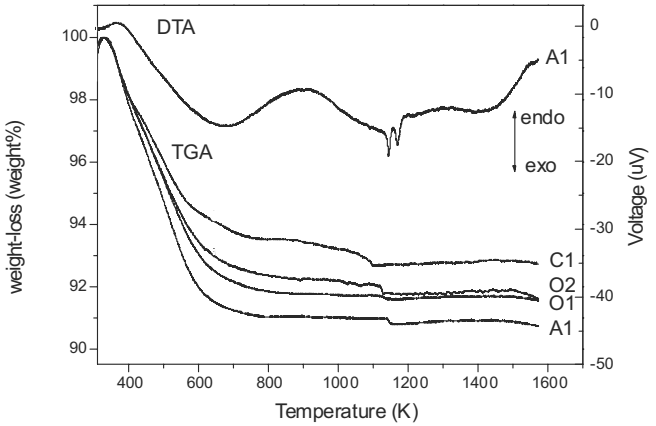

Fig. 5. Thermogravimetric analysis of sample A1, sample C1, sample O1 and, sample O2 (lower graphs) and differential thermoanalysis of sample A1 (upper graph).

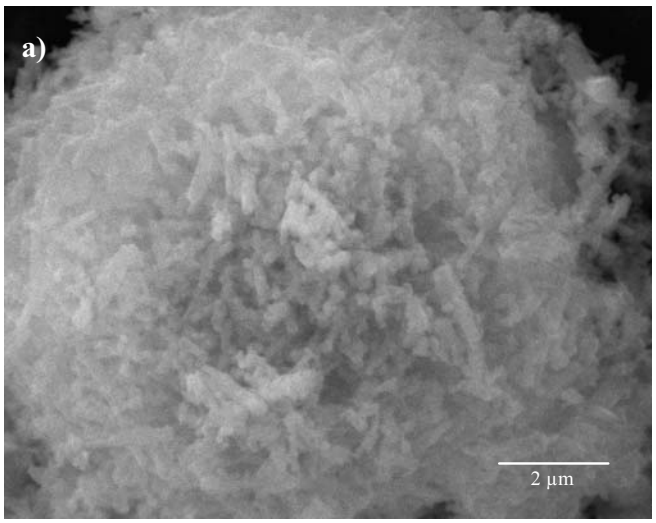

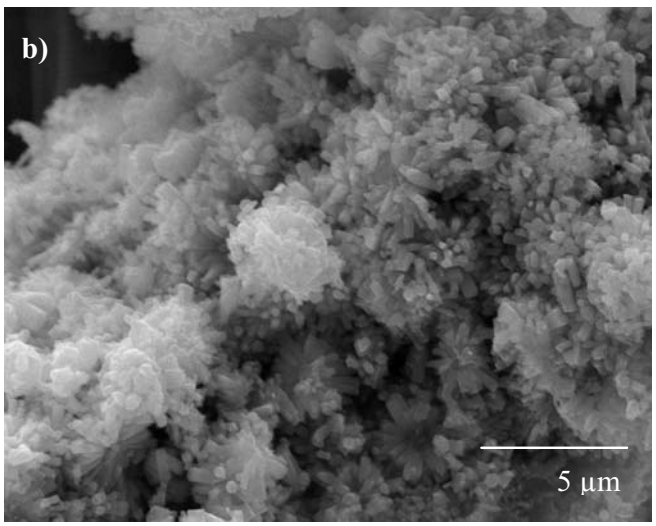

Fig. 6. SEM micrographs of a) sample A1 and b) sample O1.

bon content because salt-anions such as carbonate are usually blocking the cancrinite channels and prevent technical application (Barrer *et al.*, 1970; Buhl, 1991; Burton *et al.*, 1999; Hackbarth *et al.*, 1999). All four samples show low carbon content in the range of 0.3 wt% C (Table 2). For comparison, the carbon content of a fully occupied carbonate cancrinite is 1.2 wt% C (Hackbarth *et al.*, 1999). In addition, our synthetic cancrinite has a considerably lower carbon content than cancrinites synthesized by Burton *et al.* (1999; 0.71 wt% C). Thus, the products can be regarded as carbonate-free cancrinites, to a first approximation.

Thermogravimetry

Thermogravimetric analyses of all samples show a decreasing total weight loss with increasing reaction time as depicted in Fig. 5. The weight-loss occurs in two separate stages. The slope shows strong similarities to the thermal weight-loss of basic hydrosodalite studied by Felsche & Luger (1987). The first step between 350 and 1000 K can be interpreted as the loss of water molecules located in the channel and the ε-cages. Thermogravimetric analyses of carbonate cancrinite by Buhl (1991) showed that this compound was dehydrated at temperatures as low as 700 K. The next step of weight-loss between 1000 and 1300 K can be assigned to the decomposition of two hydroxyl anions (in combination with sodium) which decompose to a water molecule and disodium oxide ($2NaOH \Rightarrow Na_2O + H_2O$). As known from high temperature X-ray powder diffraction the cancrinite decomposes to a nepheline-like phase in the same temperature range at approximately 1000–1200 K. The decomposition can be well observed by differential thermoanalysis (Fig. 5, upper graph), which shows a two step strong exothermic reaction at this temperature. Samples O1 and O2 indicate the highest water content. Sample C1, which was prepared from precipitated silica, shows the lowest weight-loss (see Table 2). In addition, this sample shows a higher carbon content as compared to samples O1 and O2. Thus, the lower water content can be interpreted as a consequence of partial blocking of the pores by carbonate.

Scanning electron micrographs

The scanning electron micrographs of samples A1 and C1 synthesized with direct reactants exhibit more accumulation of small crystalline material in larger aggregates (Fig. 6a). The samples O1 and O2 formed from sol-gels (Fig. 6b) show well-formed hexagonal needle shape crystals intergrown in large bundles. The average grain size is 2–5µm in all samples.

^{29}Si, ^{27}Al and ^{23}Na MAS NMR spectroscopy

The ^{29}Si MAS NMR spectra show signals between –87.2 ppm and –89.2 ppm. Fig. 7 shows the spectra of samples A1 and O1. The isotropic shift is mainly determined by the $Si(OAl)_4$ tetrahedral angle and thus indirect correlated to the lattice parameters (Engelhardt *et al.*, 1989). A second broad resonance with low intensity and centre of gravity at –94.5 ppm can be observed in the base of the cancrinite sig-

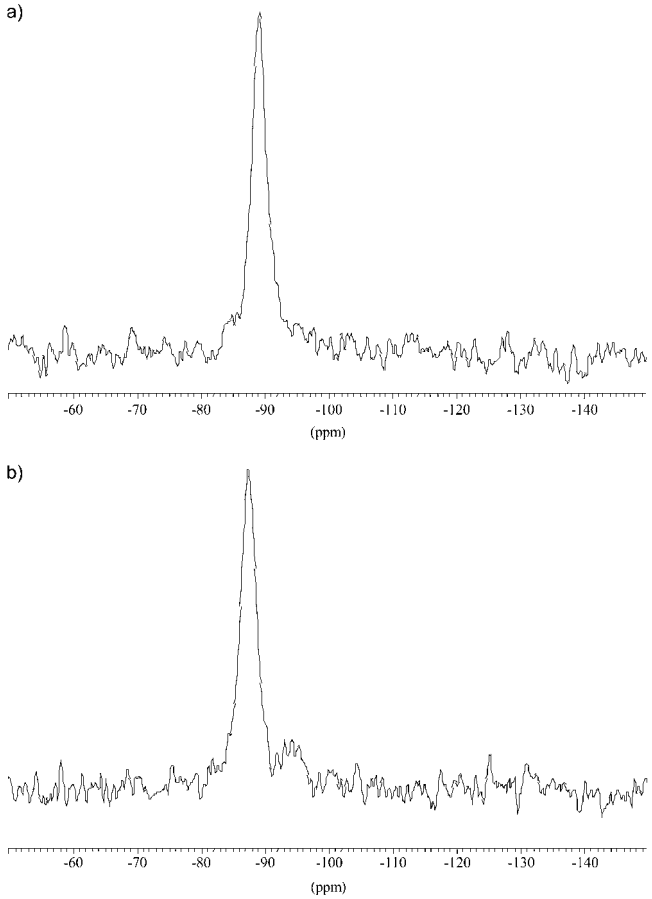

Fig. 7. ^{29}Si MAS NMR spectra of a) sample A1, and b) sample O1.

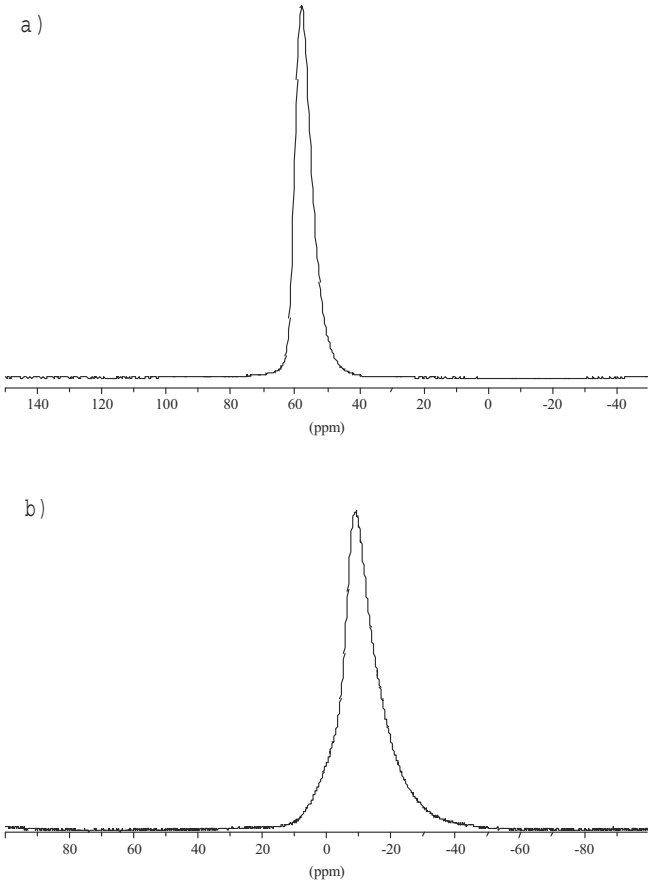

Fig. 8. ^{27}Al MAS NMR spectrum of a) sample A1, and b) ^{23}Na MAS NMR spectrum of sample C1.

nal of sample O1 which is most probably due to unreacted sol-gel component, but was not detected in the X-ray powder pattern possibly due to the amorphous character of the sol-gel. An interpretation as a slightly increased Si/Al ratio and therefore due to a Q^4(3Al) signal is inconsistent with the structure refinement data as given below. However, although the nominal Si/Al ratio of starting materials for all four samples was five, the ^{29}Si MAS NMR spectra indicate that the framework consists of completely ordered SiO_4 and AlO_4 tetrahedra with a Si/Al ratio of one. This is in contrast to the findings of Milestone *et al.* (1993) and Liu *et al.* (1995), who found an increased Si/Al ratio of 2.5–10 in the cancrinite product.

The ^{27}Al MAS NMR spectra show a single tetrahedral signal between 57.7 and 58.5 ppm. Fig. 8a shows the spectrum of sample A1 as an example. Resonances from octahedral coordinated aluminium which would resonate in the range of +15 to –15 ppm were not observed in any of the spectra. This means that cationic Al^{3+} in the sodium-free sol-gels, which is necessary to balance the charge of the amorphous network (Fechtelkord *et al.*, 2001a) is fully introduced into the cancrinite framework.

The ^{23}Na MAS NMR spectra contain an asymmetric resonance with shifts between –9.1 ppm and –10.4 ppm. Fig. 8b shows the spectrum of sample C1. A distinction between the two crystallographic positions in the ε-cages and twelve-membered ring channel in the ^{23}Na MAS NMR spectra is not possible due to the similar local environment of the sodium sites coordinated to water molecules (Fechtelkord *et al.*, 2001b).

^{1}H MAS and {^{1}H} ^{13}C CPMAS NMR spectroscopy

All ^{1}H MAS NMR spectra (Fig. 9a) are dominated by the broad resonance with maximum at approximately 4 ppm and have shoulders on the low and high field side of the signal maximum. The most distinct shoulder is observed at approximately 3 ppm. The lineshape can be explained by a superposition of the two contributions from water molecules in the channels and ε-cages and from hydroxyl-groups located in the channels. The corresponding signals are usually present at approximately 3.4 ppm and 4.3 ppm, respectively (Fechtelkord *et al.*, 2001b; Fechtelkord *et al.*, 2001c; Yesinowski *et al.*, 1988). The spectra of the cancrinites synthesized from sol-gels (*e.g.*, sample O2, Fig. 9b) have a resonance at 3.3 ppm of higher intensity than the spectra of cancrinites synthesized from direct reactants so that the two contributions can be clearly distinguished. The higher water content of the samples O1 and O2 is thought to be the source for the changed intensity ratio in those ^{1}H MAS NMR spectra. Proton resonances from methyl or methylen groups were not observed; therefore the inclusion of organic compounds into the cancrinite can be excluded.

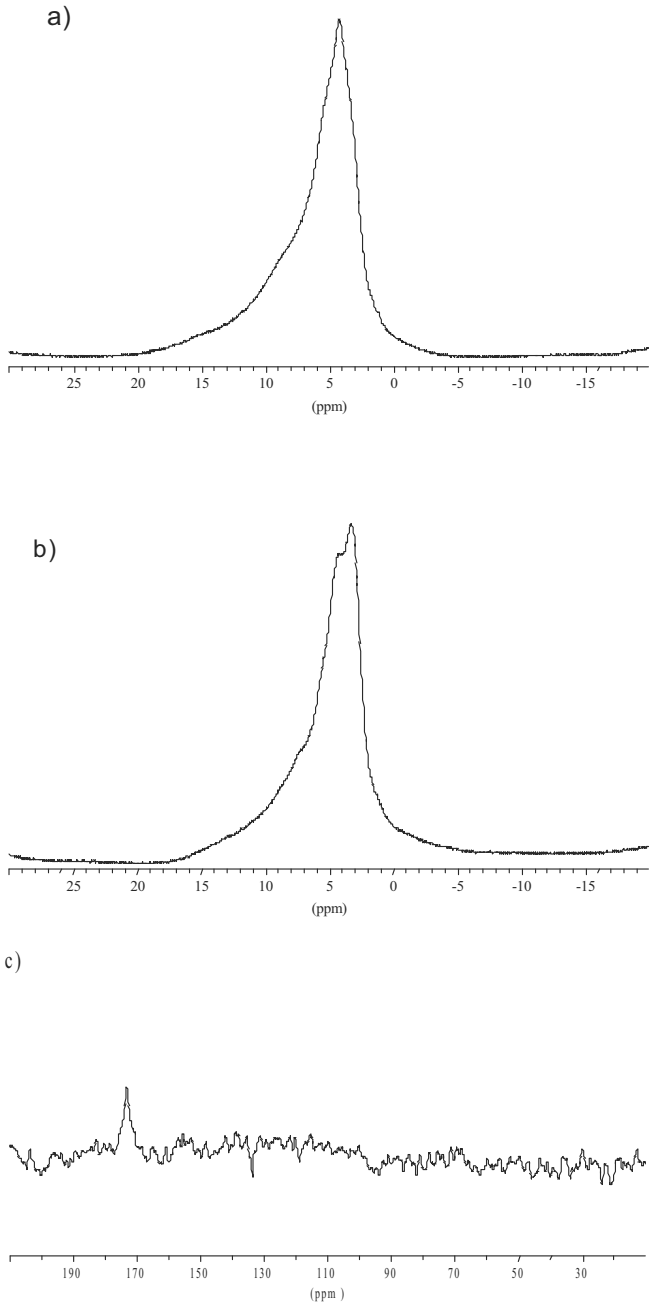

Fig. 9. ^{1}H MAS NMR spectra of a) sample A1, b) sample O2, and c) {^{1}H} ^{13}C CPMAS NMR spectrum of sample O1.

The {^{1}H} ^{13}C CPMAS NMR spectrum of sample O1 in Fig. 9c shows only resonances of small intensity at ≈170 ppm which indicates a low carbon content, and characterizes the lineshape appearance of all four {^{1}H} ^{13}C CPMAS NMR spectra. This weak signal is caused by carbonate impurities (Fechtelkord, 1999; Fechtelkord *et al.*, 2001c). Resonances from carbon atoms of other organic compounds, especially methyl and methylen carbon atoms were not detected (10–50 ppm).

Table 3. Crystal data and details of experimental powder X-ray diffraction and structure refinement.

	basic cancrinite $Na_{7.46}[AlSiO_4]_6(OH)_{1.56}(H_2O)_{7.98}$
Crystal data:	
crystal system	hexagonal
space group	$P6_3$
Z	1
a_0	12.7558(3) Å
c_0	5.1985(2) Å
M	1037.72 g/mol
V	732.52(4) Å^3
T	296 K
ρ	2.352 g/cm^3
X-ray data collection:	
2-Theta range:	$7° < 2\theta < 96.7°$
step width:	0.00777
Rietveld refinement:	
contributing reflections	295
Parameters varied in final cycle	39
Δ/σ	< 0.01
R_{wp}	0.0162
R_p	0.0107
R_{exp}	0.0095
$R(F^2)$	0.0373
DWd	1.984
χ^2	2.950
$\Delta\rho_{max}$	+0.35 e / Å^3
$\Delta\rho_{min}$	-0.24 e / Å^3

Table 4. Atomic parameters of basic cancrinite (sample C1) at T = 296 K.

Atom	$P6_3$	occupancy	x	y	z	U_{iso}
Na(1)	2b	1.0	0.333	0.667	0.637(5)	0.008(5)
Na(2)	6c	0.91(1)	0.144(3)	0.2890(8)	0.288(4)	0.032(3)
Si(1)	6c	1.0	0.0803(15)	0.4166(15)	0.75*	0.0045(11)†
Al(1)	6c	1.0	0.3333(17)	0.4132(16)	0.753(7)	0.0045
O(1)	6c	1.0	0.200(3)	0.4026(10)	0.687(4)	0.015(2)†
O(2)	6c	1.0	0.1215(8)	0.560(4)	0.749(5)	0.015
O(3)	6c	1.0	0.0452(22)	0.3666(27)	0.062(6)	0.015
O(4)	6c	1.0	0.3328(28)	0.3562(27)	0.058(8)	0.015
OH2(1)	6c	0.42(1)	0.132(6)	0.106(6)	0.983(23)	0.058(15)†
OH2(2)	6c	0.52(1)	0.095(5)	0.093(3)	0.795(13)	0.058
OH(1)	2a	0.78(1)	0	0	0.112(7)	0.018(15)
OH2(3)	6c	0.39(1)	0.621(5)	0.2907(4)	0.683(7)	0.021(17)

*Coordinate was kept fixed.
†Displacement parameters of Si(1) and Al(1), O(1), O(2), O(3) and O(4), OH2(1) and OH2(2) were restrained to be equal.

Structure refinement of sample C1

X-ray powder patterns, spectroscopic investigations, and estimated carbon and water contents suggest a cancrinite structure containing mainly Na, water, and hydroxyl anions and only minor amounts of carbonate. The ^{29}Si MAS NMR spectra indicate a strongly ordered alternating framework structure of all four samples. Sample C1, which shows the

Table 5. Selected interatomic distances (Å) and angles (deg) for the basic cancrinite (sample C1) at T = 296 K.

Atoms	Distance / Å	Atoms	Angle / deg
Si(1)-O(1)	1.66(4)	O(1)-Si(1)-O(2)	109(1)
Si(1)-O(2)	1.60(4)	O(1)-Si(1)-O(3)	104(1)
Si(1)-O(3)	1.70(4)	O(1)-Si(1)-O(4)	108(2)
Si(1)-O(4)	1.58(4)	O(2)-Si(1)-O(3)	107(2)
Average:	*1.63*	O(2)-Si(1)-O(4)	116(2)
		O(3)-Si(1)-O(4)	112(2)
		Average:	*109.3*
Al(1)-O(1)	1.67(4)	O(1)-Al(1)-O(2)	108(1)
Al(1)-O(2)	1.72(5)	O(1)-Al(1)-O(3)	114(2)
Al(1)-O(3)	1.74(3)	O(1)-Al(1)-O(4)	111(2)
Al(1)-O(4)	1.74(4)	O(2)-Al(1)-O(3)	114(2)
Average:	*1.72*	O(2)-Al(1)-O(4)	108(2)
		O(3)-Al(1)-O(4)	101(2)
		Average:	*109.3*
Na(1)-O(1)	3x 2.93(1)		
Na(1)-O(2)	3x 2.413(9)		
Na(1)-OH2(3)	3x 2.42(3)		
Na(1)-OH2(3)	3x 2.90(3)		
Na(2)-O(1)	2.42(2)		
Na(2)-O(3)	2.28(5)		
Na(2)-O(3)	3.02(5)		
Na(2)-O(4)	2.43(5)		
Na(2)-O(4)	2.84(5)		
Na(2)-OH2(1)	2.76(9)		
Na(2)-OH2(1)	2.07(9)		
Na(2)-OH2(2)	2.22(5)		
OH2(1)-OH2(2)	1.06(9)		
OH2(1)-OH2(2)	2.03(9)		
OH2(1)-OH(1)	1.69(8)		
OH2(2)-OH(1)	2.03(5)		
OH2(2)-OH(1)	1.53(6)		

best crystallinity of all four samples, has been used in the Rietveld structure refinement of cancrinite.

The cancrinite structure refinement was performed in the hexagonal space group $P6_3$. The Pseudovoigt function described by Howard (1982) and Thompson *et al.* (1987) was used as the profile function. A linear interpolation function with 36 variable parameters was used as background function. In addition, 39 fixed background points were introduced. The profile parameters were refined in the Le Bail intensity extraction mode. The hydroxylcancrinite structure model of Hassan & Grundy (1991) served as the starting model for the refinement. Restraints were set for the Si-O bond length (1.61 Å ± 0.05 Å) and the Al-O bond length (1.72 Å ± 0.05 Å). The restraint factor was decreased to 100 in the last few cycles.

In the first few cycles the framework atom positions were refined. The z-coordinate of the Si(1) position was kept fixed. After that, the atomic positions of Na, the hydroxyl oxygen atoms, and water oxygen atoms were refined. Finally, the occupancies of sodium, the OH^- and H_2O oxygen atoms were refined as well as their displacement factors, in separate cycles. The refinement converged with R_{wp} = 0.0162 (R-value of weighted profile), R_p = 0.0107 (R-value of profile) and $R(F^2)$ = 0.0373 (R-value of Bragg reflections). All crystal and experimental data are given in Table 3. The powder pattern, the Bragg positions, and the difference pattern are depicted in Fig. 1. Atomic parameters are given in Table 4 and selected atomic distances and angles in Table 5[1]. Bond-valence summations around the framework atoms Si and Al as well as the framework oxygen atoms give values which are in good agreement with the theoretical values (Brese & O'Keefe, 1991; Brown & Altermatt, 1985). The bond-valence value of 0.83 vu for the Na(2) position shows a small deviation from the theoretical value but for the Na(1) position a value of 0.99 vu is in good agreement with the theory.

On the one hand the final structure (Fig. 10) differs from that refined by Hassan & Grundy (1991). The occupancy factors of the oxygen positions OH2(1) and OH2(2) are twice as high and the second position is shifted in its x and y coordinates. The occupancy factors in the refinement of Hassan & Grundy (1991) were constrained based on results of chemical analysis. On the other hand, the occupancy factors are quite similar to the structure proposed by Barrer *et al.* (1970) and Pahor *et al.* (1982). However, it is not possible to detect which of the refined oxygen positions in the

[1] Further information of crystal structure refinement can be requested from Fachinformationszentrum Karlsruhe, D-76344 Eggenstein-Leopoldshafen under CSD-No. 411486.

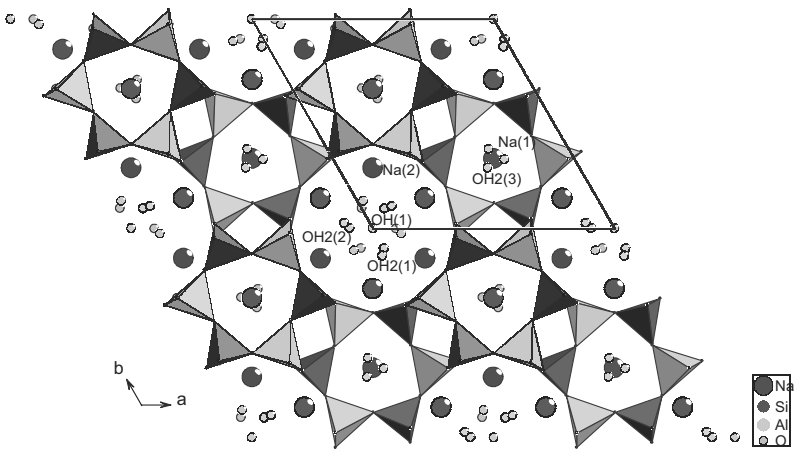

Fig. 10. Structural plot of the refined hydroxylcancrinite in the space group $P6_3$.

channel are related to water molecules and which to hydroxyl anions. Thus, from the refined occupancy factors we assigned the oxygen centre Wyckoff 2a position (OH(1)) to the hydroxyl anion and the 6c positions (OH2(1) and OH2(2)) to the water molecules. The occupancy factor (0.42) of OH2(1) (Wyckoff 6c position) is close to the theoretical value of 0.33 for two hydroxyl anions per unit cell and could also be due to the hydroxyl anion position. The OH2(1) oxygen position directly coordinate the location of Na in the channel.

The water content estimated from the refinement is 13.6 wt% H_2O which is much higher than the water content estimated by thermogravimetry (see Table 2). There may be several possible reasons for this difference: first, the channel positions are mainly occupied by water, but the hydrogen positions are not included in the refinement, this will yield too high electron density for the remaining oxygen atoms and therefore overestimate the occupancies. Second, the high degree of motion of the water molecules induces mobility of oxygen electron density in the channel. Thus, the refinement of the water positions and occupancies is difficult and probably overestimates occupancies. Finally, the IR and $\{^1H\}$ ^{13}C CPMAS NMR spectroscopic results indicate the presence of carbonate impurities. The amount was too small to introduce these carbonate positions into the structure and to refine them. However, they contribute to the electron density and also increase the calculated occupancies of the water oxygen positions. Our structure is significantly different from the structure refined by Burton *et al.* (1999). They refined the structure of a cancrinite synthesized in butanediol and found that carbonate anions occupied channel which is not detected in the present results.

Conclusions

The characterization of the four cancrinite samples shows that the synthesis of a hydroxyl cancrinite with high water content was successful. The estimated carbon content is low. The cancrinite structure can be regarded as "template-free", which could be of high interest for further technical applications. Although an initial Si/Al-ratio of five was introduced into the synthesis, the resulting Si/Al ratio of the cancrinites is one. This stands in contrast to the results of Liu *et al.* (1993) and Milestone *et al.* (1995). The Rietveld structure refinement revealed a cancrinite framework structure characterized by channels filled with water molecules and hydroxyl groups. It should be possible to remove the hydroxyl groups by washing as already known for basic hydrosodalites (Felsche & Luger, 1987). After final dehydration the cancrinite should have zeolitic properties. The refined structure presents a new structure type for Na-cancrinites synthesized in a butanediol-water system that is similar to a synthetic Cs-Li cancrinite synthesized in the same solvent mixture (Fechtelkord *et al.*, 2001c) but differs from the previous published structure of cancrinite synthesized in butanediol (Burton *et al.*, 1999).

Acknowledgements: The authors thank Dr. B. Marler (Bochum) for the data collection of the X-ray powder diffraction pattern used in the Rietveld refinement, Dr. T. Giesenberg (Hannover) for the thermogravimetric analysis data and appreciate the support of M. Strelzig (Hannover) in the synthesis and characterization of the cancrinite material. The authors are indebted to Dr. T. Gesing (Hannover) for the collection of X-ray powder diffraction data at elevated temperatures. Financial support of the project by the Deutsche Forschungsgemeinschaft (Fe486/1-2) is gratefully acknowledged. M. Fechtelkord thanks the Alexander-von-Humboldt Foundation for a Feodor Lynen research fellowship.

References

Barnakov, Y.A., Voronina, A.A., Efimov, A.N., Poborchii, V.V., Sato, M. (1995): One-dimensional selenium chain in the channel of the incommensurate cancrinite matrix. *Inorganic Materials*, **31**, 748-751.

Barrer, R.M., Cole, J.F., Villiger, H. (1970): Chemistry of soil minerals. Part VII. Synthesis, properties and crystal structure of salt-filled cancrinites. *J. Chem. Soc.,* **Series A**, 1523-1531.

Bibby, D.M. & Dale, M.P. (1985): Synthesis of silica-sodalite from non-aqueous systems. *Nature*, **317**, 157-158.

Bogomolov, V.N., Efimov, A.N., Ivanova, M.S., Poborchii, V.V., Romanov, S.G., Smolin, Y.I., Shepelev, Y.F. (1992): Structure and optical-properties of a one-dimensional selenium-atom chain in a cancrinite channel. *Fizika Tverdogo Tela*, **34**, 1722-1728.

Brandenburg, K. (2001): DIAMOND. Program for Crystal structure drawing. Version 2.1e, Crystal Impact GbR.

Brese, N.E. & O'Keefe, M. (1991): Bond-valence parameters for solids. *Acta Cryst.,* **B47**, 192-197.

Brown, I.D. & Altermatt, D. (1985): Bond-valence parameters obtained from a systematic analysis of the inorganic crystal structure database. *Acta Cryst*., **B41**, 244-247.

Buhl, J.-C. (1991): Synthesis and characterization of the basic and non-basic members of the cancrinite-natrodavyne family. *Thermochimica Acta*, **178**, 19-31.

Burton, A., Feuerstein, M., Lobo, R.F., Chan, J.C.C. (1999): Characterization of cancrinite synthesized in 1,3-butanediol by Rietveld analysis of powder neutron diffraction data and solid-state ^{23}Na NMR spectroscopy. *Microp. Mesop. Mater.*, **30**, 293-305.

Engelhardt, G., Luger, S., Buhl, J.-C., Felsche, J. (1989): ^{29}Si MAS NMR of aluminosilicate sodalites: Correlations between chemical shifts and structure parameters. *Zeolites*, **9**, 182-186.

Fechtelkord, M. (1999): Structural study of $Na_8[AlSiO_4]_6(CO_3)_x(HCOO)_{2-2x}(H_2O)_{4x}$, $0.2 \le x \le 1$ synthesized in organic solvents: Order and disorder of carbonate and formate anions in sodalite. *Microp. Mesop. Mater.,* **28**, 335-351.

Fechtelkord, M., Posnatzki, B., Buhl, J.-C. (2001a): Synthesis of basic cancrinite in a butanediol-water system. *Chem. Mater.,* **13**, 1967-1975

Fechtelkord, M., Stief, F., Buhl, J.-C. (2001b): Sodium cation dynamics in nitrate cancrinite: A low and high temperature ^{23}Na and ^1H MAS NMR-study and high temperature Rietveld structure refinement. *Am. Mineral.*, **86**, 165-175.

Fechtelkord, M., Posnatzki, B., Buhl, J.-C., Fyfe, C.A., Groat, L.A., Raudsepp, M. (2001c): Characterization of synthetic Cs-Li cancrinite grown in a butanediol-water system: An NMR spectroscopic and Rietveld refinement study. *Am. Mineral.*, **86**, 881-888.

Felsche, J. & Luger, S. (1987): Phases and thermal decomposition characteristics of hydro-sodalites $Na_{6+x}[AlSiO_4]_6(OH)_x{\cdot}n\ H_2O$. *Thermochimica Acta*, **118**, 35-55.

Flanigen, E.M., Khatami, H., Szymanski, H. (1971): Infrared struc-

tural studies of zeolite frameworks. *Adv. Chem. Ser., Molecular Sieves Zeolites,* **101**, 201-229.

Grundy, H.D. & Hassan, I. (1982): The crystal structure of a carbonate-rich cancrinite. *Can. Mineral.,* **20**, 239-251.

Hackbarth, K., Gesing, T.M., Fechtelkord, M., Stief, F., Buhl, J.-C.(1999): Synthesis and crystal structure of carbonate cancrinite $Na_8[AlSiO_4]_6CO_3(H_2O)_{3,4}$, grown under low-temperature hydrothermal conditions. *Microp. Mesop. Mater.,* **30**, 347-358.

Hassan, I. & Grundy, H.D. (1991): The crystal structure of basic cancrinite, ideally $Na_8[Al_6Si_6O_{24}](OH)_2\ 3H_2O$. *Can. Mineral.,* **29**, 377-383.

Howard, C.J. (1982): The approximation of asymmetric neutron powder diffraction peaks by sums of gaussians. *J. Appl. Cryst.*, **15**, 615-620.

Jarchow, O. (1965): Atomanordnung und Strukturverfeinerung von Cancrinit. *Z. Krist.,* **122**, 407-422.

Kanepit, V.N. & Rider E.E. (1995): Neutron diffraction study of cancrinite. *J. Struct. Chem.,* **36**, 763-765.

Kozlov, A.M., Galitskii, V.Y., Volkov, V.V., Dem'yanets, L.N., Kosova, T.B. (1989): Pyroelectric and dielectric properties of cancrinite. *Fizika Tverdogo Tela*, **31**, 39-45.

Larson, A.C. & von Dreele, R.B. (1985): GSAS – General Structure Analysis System. Los Alamos National Laboratory, Los Alamos.

Lindner, G.G., Massa, W., Reinen, D. (1995): Structure and properties of hydrothermally synthesized thiosulfate cancrinite. *J. Solid State Chem.*, **117**, 386-391.

Lindner G.G., Hoffmann, K., Witke, K., Reinen, D., Heinemann, Ch., Koch, W. (1996): Spectroscopic properties of Se_2^{2-} and Se_2^{-} in Cancrinite. *J. Solid State Chem.,* **126**, 50-54.

Liu, C., Li, S., Tu, K., Xu, R. (1993): Synthesis of cancrinite in butane-1,3-diol systems *J. Chem. Soc., Chem. Commun.*, 1645-1646.

Meier, W.M. & Olson, D.H. (1992): Atlas of Zeolite Structure Types, Structure Commission of the International Zeolite Association, Butterworth-Heinemann, London.

Milestone, N.B., Hughes, S.M., Stonestreet, P.J. (1995): Synthesis of Zeolites in Anhydrous Glycol Systems. *Stud. Surf. Sci. Catal.,* **98**, 42-43.

Nadezhina, T.N., Rastsvetaeva, R.K., Pobedimskaya, E.A., Khomyakov, A.P. (1991): Crystal structure of natural hydroxyl-containing cancrinite. *Kristallografiya,* **36**, 591-595.

Pahor, N.B., Calligaris, M., Nardin, G., Randaccio, L. (1982): Structure of a basic cancrinite. *Acta Cryst.*, **B38**, 893-985.

Poborchii, V.V., Ivanova, M.S., Ruvimov, S.S., (1994): Polarized absorption and raman-spectra of 1-dimensional selenium chains in mordenite and cancrinite single-crystals. *Stud. Surf. Sci. Catal.*, **84**, 2285-2293.

Schüth, F. (1995): Nanoporous crystals as multipurpose host matrices. *Chemie in unserer Zeit*, **29**, 42-52.

Thompson, P., Cox, D.E., Hastings, J.B. (1987): Rietveld refinement of Debye-Scherrer synchrotron X-ray data from Al_2O_3. *J. Appl. Cryst.*, **20**, 79-83.

Yesinowski, J.P, Eckert, H., Rossman, G.R. (1988): Characterization of hydrous species in minerals by high-speed ^1H MAS-NMR. *J. Am. Chem. Soc.*, **110**, 1367-1375.

Received 2 August 2001
Modified version received 24 April 2002
Accepted 29 November 2002